water

MDPI

Article

Source of Methanogens and Characteristics of Methane Emission in Two Wastewater Treatment Plants in Xi'an

Dianao Zhang [1], Huijuan Li [1,2,*], Xia Li [1], Dong Ao [1] and Na Wang [3]

[1] School of Environmental and Chemical Engineering, Xi'an Polytechnic University, Xi'an 710048, China; 230611054@stu.xpu.edu.cn (D.Z.); 220611040@stu.xpu.edu.cn (X.L.); aodong@xpu.edu.cn (D.A.)
[2] Engineering Research Center of Biological Resources Development and Pollution Control Universities of Shaanxi Province, Xi'an Polytechnic University, Xi'an 710048, China
[3] Xi'an Capital Water Co., Ltd., Xi'an 710086, China; anna1250727895@163.com
* Correspondence: hjli@xpu.edu.cn; Tel.: +86-138-9199-5434

Abstract: Methane (CH_4) is one of the potent greenhouse gases emitted from municipal wastewater treatment plants. The characteristics of methane emission from municipal wastewater treatment plants (WWTPs) have attracted lots of concern from related researchers. The present work investigated the source of methanogens and methane emission properties from two WWTPs in Xi'an, and one is employed in an Orbal oxidation ditch, and the other is anaerobic/anoxic/oxic (A/A/O). The measurement of specific methanogenic activity (SMA) and coenzyme F_{420} concentration, together with Fluorescence in situ hybridization (FISH), was used to determine the amount and activity of methanogens in two WWTPs. Additionally, a combined activated sludge model was built and predicted the growth of methanogens and other key microorganisms in the sludge. The results showed that the average CH_4 emission flux from the Orbal oxidation ditch (22.74 g CH_4 /(m^2·d)) was much higher than that from A/A/O (9.57 g CH_4/(m^2·d)). The methane emission factors in the Orbal oxidation ditch and A/A/O processes were 1.18 and 0.21 g CH_4 /(m^3 INF), respectively. These distinct methane emission characteristics between two WWTPs are mainly attributed to the higher activity and content of methanogens, as well as the discontinuous aeration in the Orbal oxidation ditch. Additionally, dissolved oxygen concentration, water temperature, and the presence of nitrate/nitrite were also important factors that influenced methane emission. The FISH analysis showed that Methanococcus was the dominant methanogen in both WWTPs. In addition, the combined model successfully simulated the growth of methanogens in WWTPs. Methanogens in WWTPs were mainly derived from the sewer system, and the cumulative effect led to an increase in the abundance of methanogens in activated sludge. The outcomes of this study provide new insights in the prediction and management of GHG emission from WWTPs.

Keywords: methane (CH_4); Orbal oxidation ditch; anaerobic/anoxic/oxic (A/A/O); wastewater treatment plant; greenhouse gases (GHGs)

check for updates

Citation: Zhang, D.; Li, H.; Li, X.; Ao, D.; Wang, N. Source of Methanogens and Characteristics of Methane Emission in Two Wastewater Treatment Plants in Xi'an. *Water* **2024**, *16*, 2101. https://doi.org/10.3390/w16152101

Academic Editor: Carmen Teodosiu

Received: 20 June 2024
Revised: 19 July 2024
Accepted: 23 July 2024
Published: 25 July 2024

Copyright: © 2024 by the authors. Licensee MDPI, Basel, Switzerland. This article is an open access article distributed under the terms and conditions of the Creative Commons Attribution (CC BY) license (https://creativecommons.org/licenses/by/4.0/).

1. Introduction

Greenhouse gases (GHGs) cause global warming, which threatens human survival. GHGs, including carbon dioxide (CO_2), methane (CH_4), and nitrous oxide (N_2O), are mainly released from human activities such as the production and consumption of fossil fuels and agricultural and industrial activities [1,2]. Among the commonly reported GHGs, CH_4 attracts more attention globally due to its 25 times higher global warming potential than CO_2 [3].

In recent years, researchers reported that wastewater treatment plants (WWTPs) are an important GHG source. The GHG emissions from WWTPs have been reported globally. Goliopoulos et al. surveyed 31 WWTPs of various sizes in Greece [4]. The annual average GHG emission, including emerging consumption, reached 207 $kgCO_{2e}$/PE, 144 $kgCO_{2e}$/PE, and 89 $kgCO_{2e}$/PE from small, medium, and large WWTPs, respectively. Aghabalaei et al.

investigated the Mashhad wastewater treatment plant [5]. The GHG emissions were 0.63 $kgCO_{2e}/m^3$. Gülşen et al. also investigated a sewage treatment plant in Turkey [6]. In China, the total GHG emissions were equal to 53.0 $MtCO_{2e}$ in 2019 [7]. Based on the Intergovernmental Panel on Climate Change (IPCC) protocol, the CO_2 emission from WWTPs is not considered as net GHG emission and thus should be excluded from the GHG inventory [8]. As a result, CH_4 and N_2O have become the key to GHG emissions from WWTPs.

Unlike N_2O generated during nitrification and denitrification under both anaerobic and oxic conditions, CH_4 is mainly produced by methanogens with low dissolved oxygen concentration and nitrite/nitrate concentration during anaerobic and/or anoxic processes [9–12]. Therefore, CH_4 emissions from WWTPs previously focused on anaerobic digesters like up-flow anaerobic sludge beds (UASBs) [6,13]. Recently, researchers also found CH_4 emission from other units in WWTPs even under oxic conditions [14–16]. These results indicated that there are different methanogens in activated sludge responsible for CH_4 generation and emission [17]. Previous studies showed that methanogens in activated sludge possibly originated from the sewer system [18]. However, limited studies have reported on CH_4 emission and microbial mechanisms, especially the amount and activity of methanogens in sludge in different WWTP units.

The carbon neutrality aims and increasingly stringent effluent standards in China require a further investigation of GHG emissions, especially CH_4 emissions from different WWTPs, to provide scientific data and technical guidelines for WWTP upgrades. In China, oxidation ditch and anaerobic/anoxic/oxic (A/A/O) processes are the most popular wastewater treatment processes and are used to treat nearly 50% of wastewater in China. Therefore, it is very important to obtain the characteristics of methane emission in these two biological nutrient removal (BNR) processes.

Some researchers employed a mathematical model to estimate GHG emissions during the design, operation, and optimization of WWTPs [19,20]. Gulhan et al. proposed a modified model based on activated sludge model No. 1 (ASM1). This model was successfully used to predict N_2O emission from a full-scale WWTP in Italy [21]. Shahabadi et al. developed a model which can simulate GHG generation in the A/A/O process [22]. Unfortunately, in spite of these research efforts, studies that focus on the source and release mechanism of methane emission from WWTPs are still limited.

The main objective of this paper is to survey CH_4 emission from two typical BNR processes (Orbal oxidation ditch and A/A/O) and investigate the factors which influence CH_4 emission. To this end, a mathematical model was developed to estimate the abundance of methanogens in two BNR processes and elucidate the release mechanism of methane emission from WWTPs.

2. Materials and Methods

2.1. Field Site

Two plants for municipal wastewater treatment in Xi'an, China, namely, the Orbal oxidation ditch process and A/A/O process, were selected. Detailed information of these plants is listed in Table 1, and a schematic of the treatment processes is shown in Figure 1.

Table 1. The operation parameters of the two plants (mg/L).

Characteristics and Parameters	Wastewater Treatment Plants (WWTPs)	
	WWTP 1	**WWTP 2**
Process	Orbal oxidation ditch	Anaerobic/Anoxic/Oxic (A/A/O)
Treatment capacity (m^3/d)	1.0×10^5	2.5×10^5

Table 1. *Cont.*

Characteristics and Parameters	Wastewater Treatment Plants (WWTPs)			
	WWTP 1		WWTP 2	
Aeration method	Surface aeration		Fine-bubble aeration	
Size (L × B × H) (m)	Anaerobic zone Oxidation ditch	27 × 9.8 × 4.95 108.2 × 50 × 4.95	Anoxic zone Anaerobic zone Oxic zone	20.3 × 50 × 6 19.3 × 50 × 6 78.7 × 50 × 6
	Influent parameters			
pH	7.0 ± 0.8		7.0 ± 0.8	
COD (mg/L)	390		380	
BOD_5 (mg/L)	200		190	
NH_4^+-N (mg/L)	20		34	
TP (mg/L)	4		4.2	
	Effluent parameters *			
pH	7.0 ± 0.8		7.0 ± 0.8	
COD (mg/L)	≤50		≤50	
BOD_5 (mg/L)	≤10		≤10	
NH_4^+-N (mg/L)	≤5		≤5	
TP (mg/L)	≤0.5		≤0.5	

Note: * Because the monitoring of two WWTP effluents only provided qualified or unqualified final results, we can only use the values of China's national standard of municipal wastewater treatment plants (GB 18918-2002, Class I-A) [23] as the effluent parameters to perform a conservative investigation.

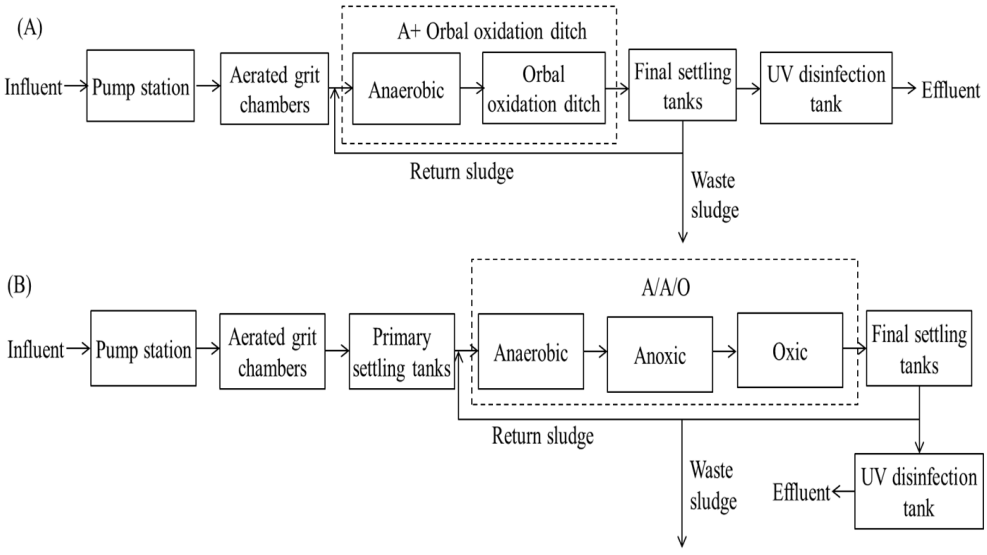

Figure 1. A simplified wastewater treatment process diagram of the two WWTPs. (**A**) WWTP 1: Orbal oxidation ditch process; (**B**) WWTP 2: A/A/O process.

2.2. The Sampling and Analysis of Methane Emission from the Two BNR Processes

2.2.1. Selecting Sampling Point

A series of sampling points were selected to investigate CH_4 emission from different wastewater treatment units in the two WWTPs. Four sample points were used in the Orbal oxidation ditch process: one sample point was set in an anaerobic tank, and the other three sample points were set in three channels of the oxidation ditch. In terms of the A/A/O process, one sample point was set in anaerobic and anoxic zones, and three sample points were set along with the water stream in the oxic zone.

All the sample points were selected close to the monitoring points of the WWTPs. On one hand, these points were representative points of each wastewater treatment. On

the other hand, other parameters, such as temperature and dissolved oxygen, could be obtained at these points during sampling processes.

In pre-experiments, the spatial variability in methane fluxes from each processing unit was examined. The results showed that CH_4 flux gradually changed with dissolved oxygen along the wastewater flow in each wastewater processing unit. In the BNR processing units with large spatial variability, gas samples were collected from multiple points, and the mean value of CH_4 fluxes was obtained. Based on data provided by the WWTPs and pre-experiment, the sample points can be used to represent different zones of the WWTPs.

2.2.2. Sample Collection

Gas samples were collected by a hand-crafted surface emission isolation flux chamber (SEIFC) with a circular cross-sectional area of 180 cm^2. The SEIFC was filled with local wastewater and was completely immersed beneath the surface of the water. Gas emitted by the reactor was left to float on the water's surface. After 2 to 3 days, gas was collected with a sampling bag. In the aerobic zone, aeration facilitated the direct and immediate collection of the gas samples. During the experiment, gas was collected every week of each month, at approximately the same time each sampling day.

CH_4 emission flux (E_{CH_4}) was calculated based on a previously reported protocol with some modification [24]. The gas flux of the aeration tank was calculated by Equation (1); the gas flux of the non-aeration tank was calculated by Equation (2). The CH_4 emission factors (ω_{CH_4}) were calculated by normalizing the total CH_4 mass flux of the BNR process to the treatment capacity (m^3 d^{-1}) and service population of the WWTP (Equations (3) and (4)).

$$E_{CH_4} = c_{CH_4} \times Q \tag{1}$$

$$E_{CH_4} = \frac{c_{CH_4} \times V_{\text{gas}}}{\Delta t \times A_{SEIFC}} \tag{2}$$

where E_{CH_4} is the CH_4 emission flux (g $CH_4/(m^2 \cdot d)$), c_{CH_4} is the CH_4 concentration in the sample (g/m^3), Q is the total diffuse air flow (m^3/d), V_{gas} is the total volume of the gas sample we collected (m^3), Δt is the time of sample collection (d), and A_{SEIFC} is the cross-sectional area of the SEIFC (0.018 m^2).

$$\omega_{CH_4,INF} = E_{CH_4} \times A_{BNR} \times \frac{1}{Q_{INF}} \tag{3}$$

$$\omega_{CH_4,person} = 365 \times A_{BNR} \times \frac{E_{CH_4}}{Q_{person}} \tag{4}$$

where $\omega_{CH_4,INF}$ is the emission factor calculated by treatment capacity (g CH_4 /(m^3 INF)), A_{BNR} is the surface of treatment units (m^2), Q_{INF} is the treatment capacity of the WWTP (m^3/d), $\omega_{CH_4,person}$ is the emission factor calculated by the population served (g $CH_4/(person \cdot year)$), and Q_{person} is the service population of the WWTP.

2.2.3. Analytical Methods

The CH_4 concentration of the gas samples was analyzed by gas chromatography (Agilent 6890 N) equipped with a Thermal Conductivity Detector (TCD) and stainless steel packed columns of TDX-01. The temperature of the injection port, detector, and land column oven was 100 °C, 160 °C, and 100 °C, respectively. Pure Ar (99.999%) was supplied as the carrier gas at a flow rate of 50 mL/min.

The dissolved oxygen (DO) concentration, pH, and water temperature of the activated sludge mixed liquor were measured on-site. Soluble chemical oxygen demand (sCOD), ammonium (NH_4^+-N), nitrate (NO_3^--N), nitrite (NO_2^--N), mixed liquor suspended solids (MLSSs), and volatile suspended solids (VSSs) were measured using APHA Standard Methods for the examination of water and wastewater [25].

2.3. Specific Methanogenic Activity and Coenzyme F_{420} Tests

The specific methanogenic activity (SMA) test is an efficient method used to determine the methanogenic activity of anaerobic sludge. F_{420}, a widely present coenzyme distributed in methanogens, is involved in CH_4 formation [26]. Both SMA and F_{420} could be used as indicators in monitoring the activity of methanogens. All batch tests were performed in triplicate. The SMA tests of acetate, propionate, and butyrate were conducted in 200 mL serum bottles at 35 ± 1 °C under anaerobic conditions. Prior to addition into the test bottles, the substrate solution was adjusted to approximately pH 7.0, and the bottles were flushed with Ar/CO_2 (80%/20%). The concentration of methane in the headspace well and the volume of biogas produced were measured every two hours because of the low gas production of the sludge. The volume of biogas accumulated in the bottle headspace was measured using gas chromatography. At the end of the tests, precise biomass was quantified through gravimetric analysis [25]. Finally, SMA was calculated according to the following equation:

$$\mu_{maxCH_4} = 4 \times \frac{dc_{CH_4} \times V_{CH_4}}{dt} \times \frac{1}{X} \quad (5)$$

where μ_{maxCH_4} is the maximum SMA [mg COD/(gVSS·d)], 4 is the conversion coefficient of CH_4 to oxygen, $\frac{dc_{CH_4} \times V_{CH_4}}{dt}$ is the CH_4 production rate (mg-CH_4/d), and X is the total biomass present in the serum bottle (g VSS).

Based on differences between the molar extinction coefficient of F_{420} under acidic and alkaline conditions, the concentration of F_{420} was measured through spectrophotometry at 420 nm. The concentration of coenzyme F_{420} was determined according to the method proposed by Wu et al. [27]. Finally, F_{420} concentration was calculated according to the following equation:

$$C_{F_{420}} = \frac{Af}{\varepsilon L x} \quad (6)$$

where $C_{F_{420}}$ is the concentration of coenzyme F_{420} in the sludge, A is the absorbance of the sample at pH 13.5 at 420 nm by comparison with the sample at a pH less than 3, f is the dilution multiple, ε is the absorbance coefficient of coenzyme F_{420} at pH 13.5 (54.3/(cm·mM)), L is the thickness of the cuvette, and x is the biomass of the sludge (g/L).

2.4. Fluorescence In Situ Hybridization

Fluorescence in situ hybridization (FISH) was used to investigate the concentration of methanogens, ammonia-oxidizing bacteria (AOB), nitrite-oxidizing bacteria (NOB), and polyphosphate-accumulating organisms (PAOs) in the two WWTPs. The rRNA-targeted oligonucleotide probes used in the experiment are presented in Table 2. During the experiments, the mixture of liquids and sludge was sampled. Then, the sludge samples were obtained after centrifugation. The sludge samples were pretreated according to the protocol described previously by Amann et al. [28]. FISH was performed according to standard protocols [25]. In brief, the hybridization buffer (Table 2) and fluorescent probe were mixed gently. Then, hybridization was performed in an equilibrated chamber. After washing in the washing buffer, rinsing with distilled water, and air drying, the slide was mounted with a drop of Citiflour (Sigma, New York, NY, USA). FISH images were collected and recorded by a laser scanning confocal microscope (Leica TCS SP8, Wetzlar, Germany).

Table 2. rRNA-targeted oligonucleotide probes used in this research.

Probe Name	Target	Sequence (5′-3′)	Formamide %	Reference
EUB 338	Eubacteria	GCT GCC TCC CGT AGG AGT	35	[29]
EUB 338II	To be used in combination with probe EUB338	GCA GCC ACC CGT AGG TGT	35	
EUB 338III	To be used in combination with probe EUB338	GCT GCC ACC CGT AGG TGT	35	
ARC 915	Archaebacteria	GTG CTC CCC CGC CAA TTC CT	35	[30]
Nso1225	Betaproteobacterial ammonia-oxidizing bacteria	CGCCATTGTATTACGTGTGA	35	[31]
NEU	Most halophilic and halotolerant	CCCCTCTGCTGCACTCTA	40 *	[32]
NmV	Nitrosococcus mobilis	TCCTCAGAGACTACGCGG	35	[33]
Cluster6a 192	Nitrosomonas oligotropha lineage	CTTTCGATCCCCTACTTTCC	35	[34]
Ntspa662	Genus Nitrospira	GGAATTCCGCGCTCCTCT	35	[34]
Nit3	Genus Nitrobacter	CCTGTGCTCCATGCTCCG	40	[35]
Nsm156	Nitrosomonas	TATTAGCACATCTTTCGAT	5	[31]
Nsv443	Nitroso-spira, -lobus, -vibrio	CCGTGACCGTTTCGTTCCG	30	[31]
PAO462	Most Accumulibacter	CCGTCATCTACWCAGGGTATTAAC	35	[36]
PAO651	Most Accumulibacter	CCCTCTGCCAAACTCCAG	35	
PAO846	Most Accumulibacter	GTTAGCTACGGCACTAAAAGG	35	

Note: * NEU can also be used with 35% FA.

2.5. Model Formation

In order to simulate the growth of methanogens accurately, a series of models was employed. First of all, anaerobic digestion models No. 1 and 2 (ADM1 and ADM 2) were used to simulate the methanogenesis with amendments. The anaerobic digestion model (ADM) [37] is commonly used to simulate anaerobic digestion, namely methanogenesis. Since our objective is to predict the CH_4 emission from processes, the ADM is necessary. Based on the results, nitrate/nitrite could also affect CH_4 generation and emission. The model to simulate nitrification, activated sludge model No. 1 (ASM1) [38], was used. In the WWTPs, phosphorus-accumulating organisms (PAOs) can cause organic compounds to compete with methanogens, also affecting CH_4 formation. Therefore, activated sludge model No. 2D (ASM2D) for phosphorus removal was merged into ASM 1. As a result, our model was established by combining ADM with ASM1 and ASM2 to obtain more accurate predictions for the growth of methanogens and CH_4 emission.

The key processes simulated in the model are shown in Figure 2. The amendments of model ADM2 [39] are as follows: (1) the equation of the acetic acid utilization process remained unchanged, the stoichiometric coefficient corresponding to methanogens in the process was set to 1, and other stoichiometric coefficients were adjusted accordingly; (2) phosphorus which was required by methanogen growth was considered; (3) the same as the decay of autotrophic or heterotrophic bacteria and PAOs, X_S (particulate biodegradable organic matter), X_P (microbial decay of a particle state product), and X_{PD} (particulate biodegradable organic phosphorus) from methanogen decay were considered; and (4) in the anoxic and aerobic tank, sludge floc can form an anaerobic environment inside the floc for methanogen growth, because bacteria outside the floc consume dissolved oxygen and nitrate. Therefore, to make the model simulate the growth of methane bacteria in anoxic and aerobic tanks, a double switch function was added to the methanogen growth kinetics equation. In the anaerobic tank, the dissolved oxygen and nitrate concentration was almost 0; then, the switching function value was 1. In the aerobic and anoxic tank, the larger the dissolved oxygen and nitrate concentration, the smaller the switching function value.

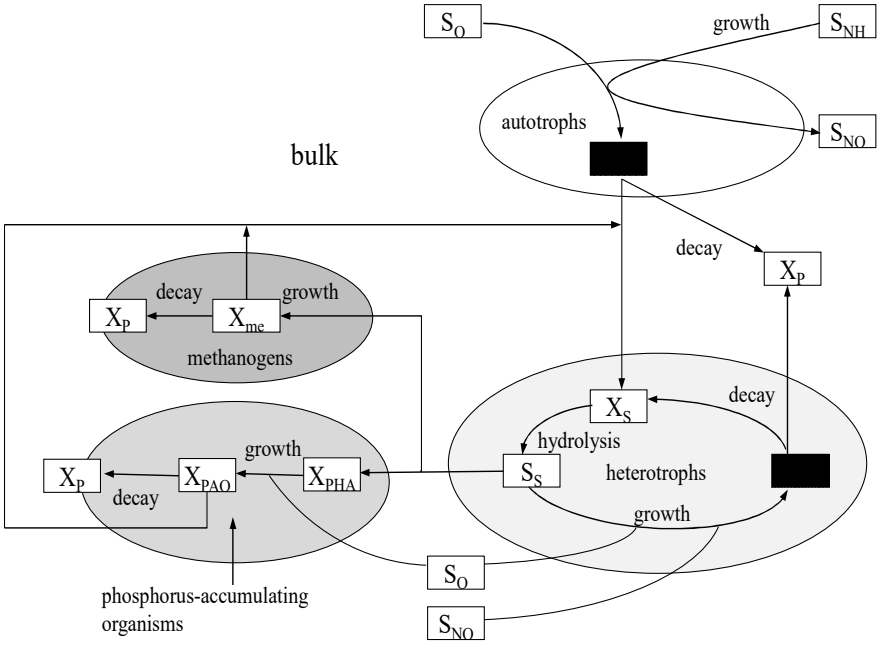

Figure 2. The conversion pathways of carbon, nitrogen, and phosphorus in the model.

ASM 1 used in our model was also modified and combined with the ADM to simulate the growth and decay of methanogens with acetic acid in WWTPs. Meanwhile, the modified ASM 1 can also simulate carbon oxidation and nitrogen removal (i.e., nitrification and denitrification). Part of the phosphorus removal of activated sludge model No. 2D (ASM2D) was combined with ASM1 [40]. In order to make the decay of phosphorus-accumulating organisms (PAOs) correspond with the decay of autotrophic and heterotrophic bacteria in ASM1, a new component X_{PD} (particulate biodegradable organic phosphorus) and a stoichiometric coefficient V_P (phosphorus content of Attenuation product) were introduced into the modified model. To make the hydrolysis of XPD correspond with the hydrolysis of X_{ND} and X_S, the hydrolysis of entrapped organophosphate was also introduced. Consequently, the ADM-modified ASM1 model can simulate methanogen growth and decay, as well as carbon oxidation and nitrogen and phosphorus removal, at the same time. The composite model matrix is shown in Table 3.

$$\mu_{m,me} \frac{S_S}{K_S + S_S} \frac{K_{OHme}}{K_{OHme} + S_O} \frac{K_{NOme}}{K_{NOme} + S_{NO}} X_{me} \tag{7}$$

where $\frac{K_{OHme}}{K_{OHme}+S_O} \frac{K_{NOme}}{K_{NOme}+S_{NO}}$ is the double switch function; K_{OHme} and K_{NOme} are the inhibition coefficients of the oxygen and nitrate of the anaerobic zone switching function coefficient inside of the sludge floc, respectively.

The total conversion rate of methanogens (X_{me}) is $r_{19} = \sum_{j=18}^{19} v_{19j}\rho_j$, where ρ_j is the kinetic equation of the j process; v_{19j} represents the corresponding stoichiometric coefficients of the X_{me} component in the process j.

Table 3. Process kinetics and stoichiometry for carbon oxidation, nitrogen, and phosphorus removal as well as the methanogens' growth.

Component i	**1**	**2**	**3**	**4**	**5**	**6**	**7**	**8**	**9**	**10**	**11**	**12**	**13**	**14**	**15**	**16**	**17**	**18**	**19**	**Process Rate ρ_j ($ML^{-3}\ T^{-1}$)**
Process j ↓	S_I	S_S	X_I	X_S	X_{BH}	X_{BA}	X_P	S_O	S_{NO}	S_{NH}	S_{ND}	X_{ND}	S_{ALK}	S_{PO4}	X_{PHA}	X_{PP}	X_{PAO}	X_{PD}	X_{me}	
1 Aerobic growth of heterotrophs		$\frac{-1}{Y_H}$			1			$-\left(\frac{1-Y_H}{Y_H}\right)$		$-i_{XB}$			$-\frac{i_{XB}}{14}$	$-i_{PBM}$						$\mu_H\left(\frac{S_S}{K_S+S_S}\right)\left(\frac{S_O}{K_{OH}+S_O}\right)X_{BH}$
2 Anoxic growth of heterotrophs		$\frac{-1}{Y_H}$			1				$-\frac{1-Y_H}{2.86Y_H}$	$-i_{XB}$			$\frac{1-Y_H}{14\times 2.86Y_H}-\frac{i_{XB}}{14}$	$-i_{PBM}$						$\mu_H\left(\frac{S_S}{K_S+S_S}\right)\left(\frac{K_{OH}}{K_{OH}+S_O}\right)\left(\frac{S_{NO}}{K_{NO}+S_{NO}}\right)\eta_g X_{BH}$
3 Aerobic growth of autotrophs						1		$-\left(\frac{4.57-Y_A}{Y_A}\right)$	$-\frac{i_{XB}}{14}-\frac{1}{7Y_A}$	$-\frac{i_{XB}}{Y_A}-$			$-\frac{i_{XB}}{14}-\frac{1}{7Y_A}$	$-i_{PBM}$						$\mu_A\left(\frac{S_{NH}}{K_{NH}+S_{NH}}\right)\left(\frac{S_O}{K_{OA}+S_O}\right)X_{BA}$
4 Decay of heterotrophs				$1-f_P$	-1		f_P					$\frac{i_{XB}}{f_P\cdot i_{XP}}$						$\frac{i_{PBM}}{f_P.v_p}$		$b_H\cdot X_{BH}$
5 Decay of autotrophs				$1-f_P$		-1	f_P					$\frac{i_{XB}}{f_P\cdot i_{XP}}$						$\frac{i_{PBM}}{f_P.v_p}$		$b_A\cdot X_{BA}$
6 Ammonification of soluble organic nitrogen										1	-1		$\frac{1}{14}$							$K_a\cdot S_{ND}\cdot X_{BH}$
7 Hydrolysis of entrapped organics		1		-1																$K_h\frac{X_S/X_{BH}}{K_X+\left(X_S/X_{BH}\right)}\left[\left(\frac{S_O}{K_{OH}+S_O}\right)+\eta_h\left(\frac{K_{OH}}{K_{OH}+S_O}\right)\left(\frac{S_{NO}}{K_{NO}+S_{NO}}\right)\right]X_{BH}$
8 Hydrolysis of entrapped organic nitrogen											1	-1								$\rho_7\left(X_{ND}/X_S\right)$
9 Storage of X_{PHA}		-1												Y_{PO4}	1	-Y_{PO4}				$q_{PHA}\cdot\frac{S_S}{K_{SS}+S_S}\cdot\frac{X_{PP}/X_{PAO}}{K_{PP}+X_{PP}/X_{PAO}}\cdot X_{PAO}$
10 Aerobic storage of X_{PP}								-Y_{PHA}						-1	-Y_{PHA}	1				$q_{PP}\cdot\frac{S_{O_2}}{K_{O_2}+S_{O_2}}\cdot\frac{S_{PO_4}}{K_{PS}+S_{PO_4}}\cdot\frac{X_{PHA}/X_{PAO}}{K_{PHA}+X_{PHA}/X_{PAO}}\cdot\frac{K_{MAX}-X_{PP}/X_{PAO}}{K_{IPP}+K_{MAX}-X_{PP}/X_{PAO}}\cdot X_{PAO}$

Table 3. *Cont.*

Component i	**1**	**2**	**3**	**4**	**5**	**6**	**7**	**8**	**9**	**10**	**11**	**12**	**13**	**14**	**15**	**16**	**17**	**18**	**19**	**Process Rate ρ_j ($ML^{-3}\ T^{-1}$)**
Process j ↓	S_I	S_S	X_I	X_S	X_{BH}	X_{BA}	X_P	S_O	S_{NO}	S_{NH}	S_{ND}	X_{ND}	S_{ALK}	S_{PO4}	X_{PHA}	X_{PP}	X_{PAO}	X_{PD}	X_{me}	
11 Anoxic storage of X_{PP}									$-\frac{1}{2.86}Y_{PAO}$					-1	-Y_{PHA}	1				$\rho_{10}\cdot\eta_{NO_3}\cdot\frac{K_{O_2}}{S_{O_2}}\cdot\frac{S_{NO_3}}{K_{NO_3}+S_{NO_3}}$
12 Aerobic growth of X_{PAO}								$-\left(\frac{1-Y_{PAO}}{Y_{PAO}}\right)$		$-i_{XB}$				$-i_{PBM}$	$\frac{-1}{Y_{PAO}}$		1			$\mu_{PAO}\cdot\frac{S_{O_2}}{K_{O_2}+S_{O_2}}\cdot\frac{S_{NH_4}}{K_{NH_4}+S_{NH_4}}\cdot\frac{S_{PO_4}}{K_P+S_{PO_4}}\cdot\frac{X_{PHA}/X_{PAO}}{K_{PHA}+X_{PHA}/X_{PAO}}\cdot X_{PAO}$
13 Anoxic growth of X_{PAO}									$-\left(\frac{1-Y_{PAO}}{2.86Y_{PAO}}\right)$	$-i_{XB}$				$-i_{PBM}$	$\frac{-1}{Y_{PAO}}$		1			$\rho_{12}\cdot\eta_{NO_3}\cdot\frac{K_{O_2}}{S_{O_2}}\cdot\frac{S_{NO_3}}{K_{NO_3}+S_{NO_3}}$
14 Lysis of X_{PHA}		1													-1					$b_{PHA}\cdot X_{PHA}$
15 Lysis of X_{PP}														1		-1				$b_{PP}\cdot X_{PP}$
16 Lysis of X_{PAO}				$1-f_P$			f_P					$\frac{i_{XB}-f_P\cdot i_{XP}}{}$					-1	$\frac{i_{PBM}-f_P\cdot v_P}{}$		$b_{PAO}\cdot X_{PAO}$
17 Hydrolysis of entrapped organic phosphorus														1				-1		$\rho_7(X_{PD}/X_S)$
18 Growth of methanogens		$\frac{-1}{Y_{me}}$												$-i_{PBM}$					1	$\mu_{m,me}\frac{S_S}{K_S+S_S}\frac{K_{OHme}}{K_{OHme}+S_O}\frac{K_{NOme}}{K_{NOme}+S_{NO}}X_{me}$
19 Decay of methanogens				$1-f_P$			f_P					$\frac{i_{XB}-f_P\cdot i_{XP}}{}$						$\frac{i_{PBM}-f_P\cdot v_P}{}$	-1	$b_{me}\cdot X_{me}$
Observed conversion rates ($mL^{-3}\ T^{-1}$)													$r_i=\sum_j v_{ij}\rho_j$							

3. Results

3.1. Methane Fluxes from the Two BNR Processes

Methane is formed in the sewer system as well as in anaerobic and anoxic processes in WWTPs due to low dissolved oxygen concentration [41]. Due to low water solubility [42], methane could be rapidly emitted from wastewater. The measured daily methane flux ranges from each unit of the two BNR processes during the experimental period are presented in Table 4. Figure 3 shows the monthly methane flux from the two BNR plants. During the period of investigation, the average CH_4 fluxes from the Orbal oxidation ditch and A/A/O processes were 22.74 and 9.57 g $CH_4/(m^2 \cdot d)$, respectively, indicating that the CH_4 flux from the Orbal oxidation ditch process was more than two times higher than that from the A/A/O process. Figure 3 shows that the Orbal oxidation ditch system emitted a significantly higher amount of methane than the A/A/O system. This result indicates that process configuration affected methane emission. Two main factors possibly influenced methane emission. Firstly, the aeration system played a key role in affecting methane emission. Continuous micropore aeration in the A/A/O process was more efficient than the intermittent surface aeration in the Orbal oxidation ditch process, resulting in higher dissolved oxygen concentration in the former one. Since all methanogens were strictly and obligatory anaerobic, high dissolved oxygen concentration could inhibit methane formation directly [43]. Secondly, the absence of a primary settling tank could allow methanogens to directly flow into the Orbal oxidation ditch with influent and thereby increase the abundance of methanogens in the Orbal oxidation ditch system.

Table 4. Methane flux range and average in each processing unit.

WWTP	Processing Unit	Methane Flux (g $CH_4/(m^2 \cdot d)$)	
		Range	Average
Orbal oxidation ditch	Anaerobic tank	10.82~24.92	18.13
	Oxidation ditch	2.79~7.45	4.61
A/A/O	Anaerobic tank	4.55~11.34	7.57
	Anoxic tank	0.39~0.89	0.65
	Oxic tank	0.77~2.19	1.35

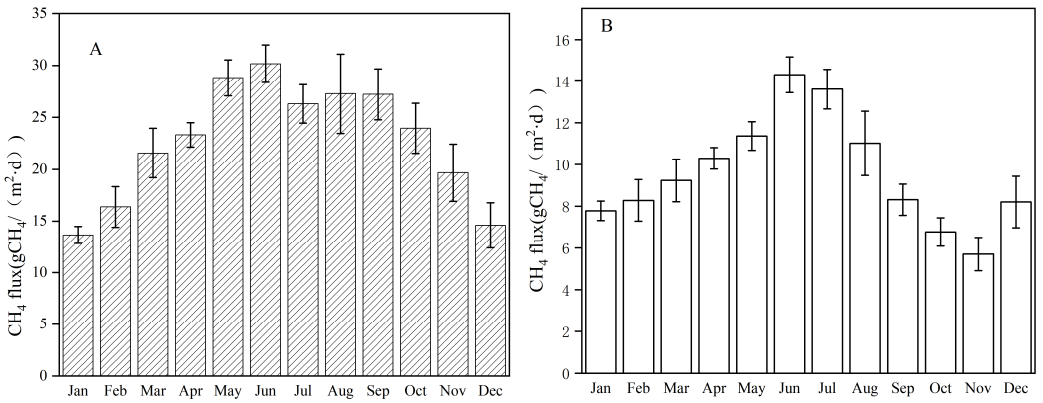

Figure 3. Emission fluxes of methane for two BNR processes. (**A**) Orbal oxidation ditch process; (**B**) A/A/O process.

Table 4 shows that the methane fluxes decreased from anaerobic tanks to oxidation ditches in the Orbal oxidation ditch process, implying that the increase in dissolved oxygen in bulk water can substantially decrease methane production. In the A/A/O process, a similar trend was observed in anaerobic/oxic/anoxic tanks. However, due to the continuous mechanical aeration stripping of dissolved methane from water in the oxic tank, the methane emission in the oxic tank was a bit higher than that in the anoxic tank. Because of the relatively higher oxidation/reduction potential (not conducive to the production of

methane) and lack of aeration stripping, the anoxic tank has the lowest methane emission in the A/A/O process.

3.2. The Methane Emission Factors of the Two BNR Processes

Emission factors were calculated by the population served and treatment capacity. For the Orbal oxidation ditch process, the per capita emission factor ranged from 39.81 g CH_4 (person·year) to 99.78 g CH_4/(person · year), and the flow-based emission factor ranged from 0.72 g CH_4/(m^3 INF) to 1.82 g CH_4 /(m^3 INF). For the A/A/O process, the range of the per capita emission factor was 7.05–18.32 g CH_4 /(person · year), and that of the flow-based emission factor was 0.13–0.33 g CH_4/(m^3 INF). The average per capita emission factors of the Orbal oxidation ditch and the A/A/O processes were 65.08 and 11.97 g CH_4/(person · year), respectively, and their average flow-based emission factors were 1.19 and 0.22 g CH_4/(m^3 INF), respectively. The emission factors of the Orbal oxidation ditch process were 5.4 times higher than that of the A/A/O process. Table 5 compares methane emission factors between our study and five other full-scale WWTPs in the literature. It can be found that A/A/O is the wastewater treatment process that releases the least methane.

Table 5. Methane emission factors from this study and other full-scale WWTPs in the literature.

WWTP	Methane Emission Factors		Reference
	g CH_4 /(m^3 INF)	g CH_4/(Person · Year)	
Orbal oxidation ditch	0.72–1.82 (1.18)	39.81–99.79 (64.67)	This study
A/A/O	0.13–0.33 (0.21)	7.05–18.32 (11.44)	
Orbal oxidation ditch	0.90–1.40 (1.2)	-	[44]
A/A/O	0.30–0.50 (0.7)	-	
Reversed A/A/O	0.30–1.00 (0.7)	-	
A/A/O	0.066–0.425	8.95–63.00	[45]
Sequencing batch reactor (SBR)	0.088–0.015	8.33–66.07	

Note: The values in brackets are the average.

3.3. SMA and Coenzyme F_{420} Tests

SMA is important in evaluating the methanogenic potential of methanogens. There are two metabolic pathways for methanogenesis, and the SMA test can indicate the rate of methanogens using different substrates. The SMA in different systems is shown in Figure 4. The SMA values of acetic, propionic, and butyric acids were 27.36, 20.64, and 23.81 mg COD-CH_4/(g VSS·d), respectively, in the Orbal oxidation ditch process, while they were 17.38, 14.12, and 14.60 mg COD-CH_4/(g VSS·d), respectively, in the A/A/O process. In our study, sludge from two BNRs can generate CH_4 via both hydrogenotrophic methanogenesis and acetoclastic methanogenesis. As a result, the methane production rate of sludge in the Orbal oxidation ditch process is higher than that in the A/A/O process.

The coenzyme F_{420} is widely observed in methanogens, and it is a key chemical involved in methanogenesis. The concentration of coenzyme F_{420} indicates the quantity and activity of methanogens in sludge. The higher concentrations of coenzyme F_{420} showed a higher activity of methanogens. The concentrations of this enzyme in the Orbal oxidation ditch and A/A/O processes were 0.0192 and 0.0134 μmol/g VSS, respectively. The methanogenic potential activity of the sludge in the Orbal oxidation ditch process was higher than that in the A/A/O process because SMA and F_{420} concentration in the former were higher than those in the latter. SMA and F_{420} concentration could also explain the high amount of methane emitted from the Orbal oxidation ditch process.

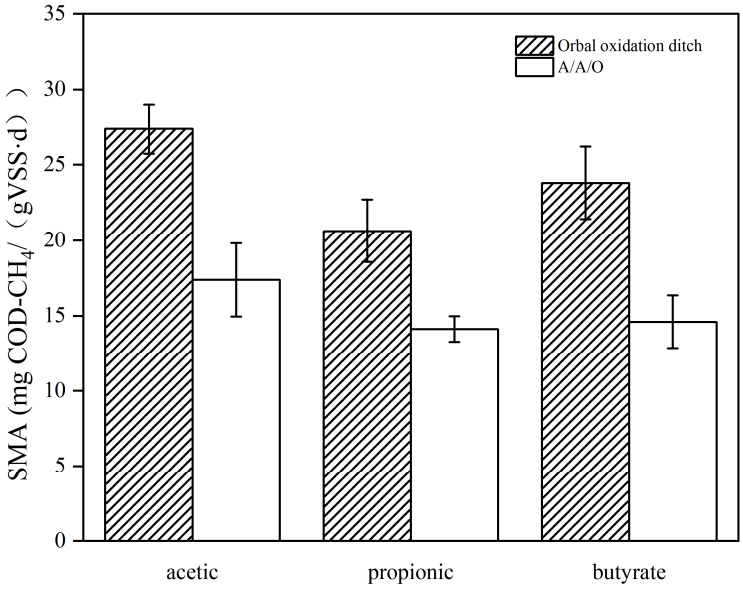

Figure 4. SMA in the two BNR WWTPs.

3.4. FISH Analysis of the Sludge from the Two WWTPs

FISH with oligonucleotide probes targeting the rRNA was used to analyze the abundance of microbial populations of the two WWTPs. As shown in Figure 5, the percentages of methanogens in the Orbal oxidation ditch process were greater than that in the A/A/O process. The number of methanogens obtained by FISH was 2.41×10^8/gVSS in the influent of the Orbal oxidation ditch process and 3.43×10^8/g-VSS in the activated sludge from the Orbal oxidation ditch process. In the A/A/O process, the number of methanogens was 1.08×10^8/gVSS in the influent and 1.93×10^8/gVSS in activated sludge. The results should be used as biological tools to explain why methane emission from the Orbal oxidation ditch process was higher than the A/A/O process.

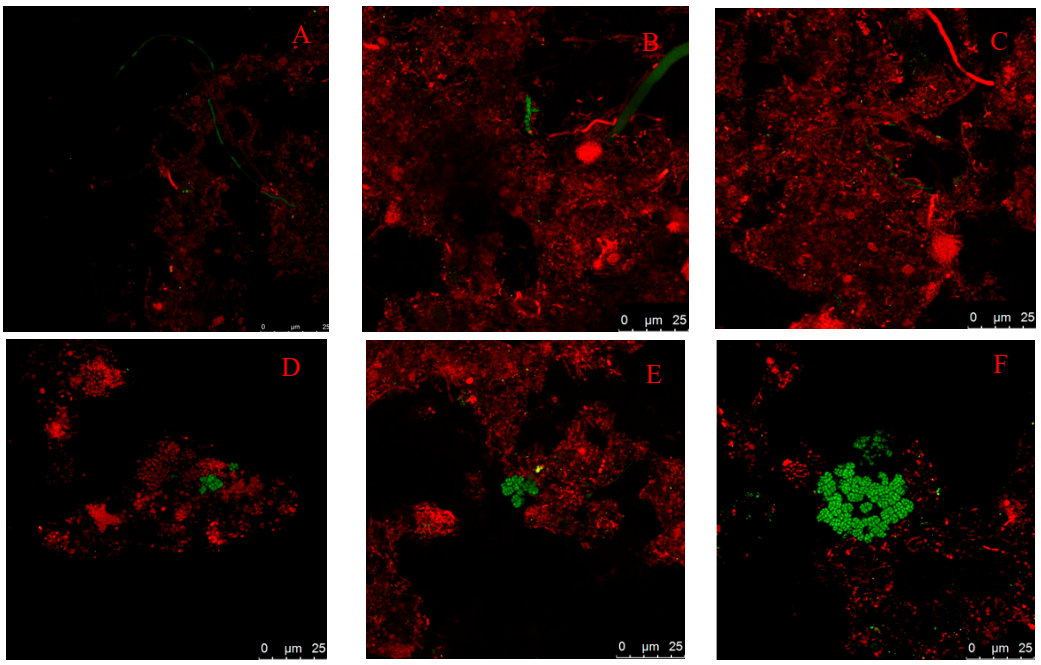

Figure 5. *Cont.*

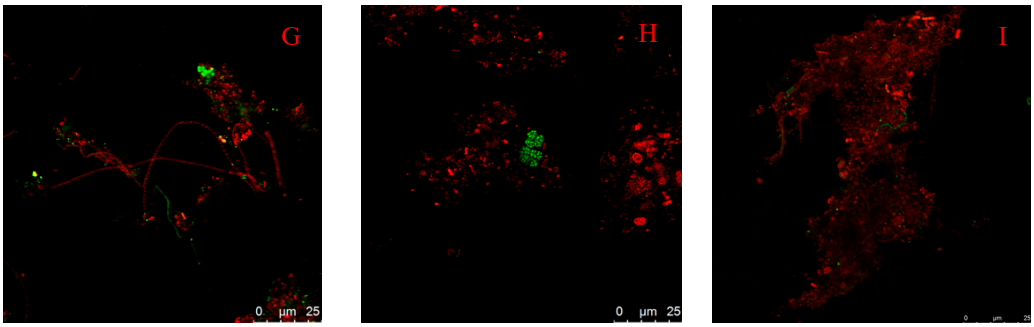

Figure 5. Fluorescent in situ hybridization of sludge from two WWTPs. (**A**–**C**) Influent of Orbal oxidation ditch process; (**D**,**E**) Influent of A/A/O process; (**F**,**G**) Orbal oxidation ditch process; (**H**,**I**) A/A/O process; red is EUB338 mix; green is ARC915; bar = 25 µm.

Most methanogens in WWTPs are from urban sewer systems. The FISH results showed that the influent of the Orbal oxidation ditch process contains Methanococcus, Methanosaeta, and Methanobacteriales, while the influent of the A/A/O process contains only Methanococcus and Methanosaeta. Methanosaeta and Methanococcus are two kinds of methanogens in activated sludge in both WWTPs, and Methanococcus are the dominant bacteria of methanogens. The relative abundance of Methanosaeta was low in both WWTPs. Meanwhile, no Methanobacteriales were found in the sludge from WWTPs. The result indicated that Methanococcus had a stronger adaptability to the environment changes than Methanosaeta and Methanobacteriales. As a result, Methanococcus became the dominant bacteria of methanogens in WWTPs.

3.5. Influencing Factors of Methane Emissions

Many studies reported that a number of factors could influence methane emission from WWTPs, such as dissolved oxygen concentration, temperature, pH, organic loading rate, and rapidly changing process conditions [46–50]. In the present study, methane emission was observed in each biological treatment unit in the two BNR processes, with anaerobic zone as the major source of methane emission. In addition, the total methane emission was larger in summer than in winter. A series of water quality parameters were analyzed to determine the main factors that influence CH_4 flux from WWTPs.

3.5.1. DO Concentration

In the A/A/O process, the amount of methane emission decreased in the following order: anaerobic tank > oxic tank > anoxic tank. The dissolved oxygen (DO) concentration (<0.18 mg/L) in the anaerobic tank was stable, leading to the conclusion that CH_4 emission from this unit has no significant change. Interestingly, the linear relationship between methane flux and dissolved oxygen concentration in the oxic tank (R^2 = 0.70) was showed in Figure 6. In general, the presence of oxygen inhibited methane formation and emission in wastewater [43]. However, in this study, the generated CH_4 was stored in the sludge floc as fine bubbles which are not able to be emitted to the atmosphere. In the oxic tank, the aeration breaks the floc down and also merges the CH_4 bubbles with air, leading to observed emission. As a result, the DO concentration in the oxic tanks had a positive impact on the methane emission rate from the zones.

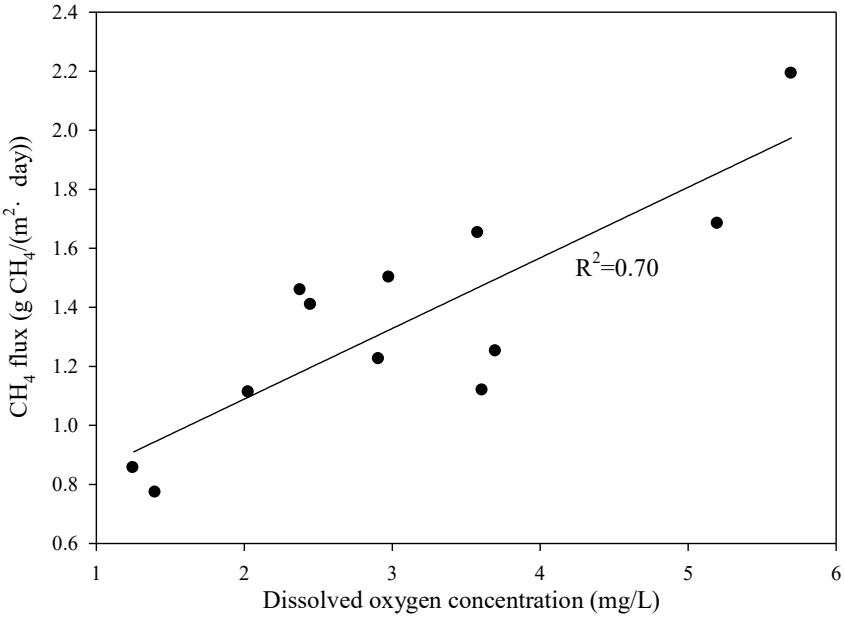

Figure 6. The relationship between methane flux and dissolved oxygen concentration in the oxic tank of the A/A/O process.

3.5.2. Temperature

In the A/A/O process, during the experimental period, wastewater temperature widely varied because of changes in air temperature. Therefore, it was necessary to determine the relationship between methane flux and water temperature. Figure 7 shows the responses of methane flux from the anaerobic zone and oxic zone to the changing of water temperature. The results of the linear regression analysis showed a statistically significant correlation between the anaerobic tank (R^2 = 0.87) and oxic tank (R^2 = 0.75); however, no statistically significant correlation was observed between methane emission and wastewater temperature in the anoxic tank (R^2 = 0.13).

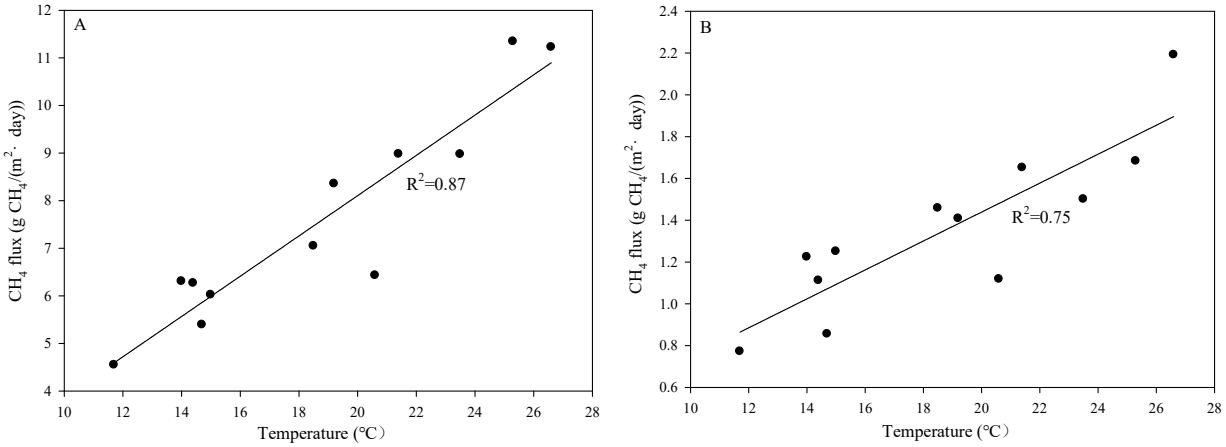

(**A**) Anaerobic tank (**B**) Oxic tank

Figure 7. Relationship between methane flux and water temperature.

3.5.3. Nitrite/Nitrate Concentration

In the A/A/O process, nitrate and nitrite concentrations in each wastewater processing tank were unstable during the experimental period. The concentration ranges of nitrate and nitrate were 1.35–8.75 mg/L and 0.05–0.22 mg/L, respectively. The coefficient of determination for CH_4 emission versus nitrate concentration in the wastewater processing

tanks was close to 0.23. The relationship between CH_4 emission and nitrite concentration had no significant correlation ($R^2 < 0.15$).

The relationship between the methane emission rate and nitrate/nitrite concentration shows a marginal correlation in the A/A/O process. But recent studies indicated that nitrite can effectively inhibit methane production in anaerobic wastewater treatment processes [51,52]. The inhibition concentration thresholds of nitrate and nitrite for methane production were about 8 mg/L and 0.07 mg/L, respectively. Nitrate and nitrite concentrations in the A/A/O process fluctuated and were lower than their corresponding inhibition concentration threshold many times. This result explained the absence of significant statistical correlations between methane emission and nitrate/nitrite concentration.

3.6. Modeling Methanogen Growth in WWTPs

Simulative and experimental results are compared in Tables 6 and 7. A composite model was employed for the estimation of methanogen growth in WWTPs. In the Orbal oxidation ditch, the relative abundance of methanogens from simulation is 3.44%, and the in situ abundance is 3.35%. Meanwhile, the relative abundance of methanogens in A/A/O is 1.92% (simulative result) and 1.95% (actual/field/in situ results). Meanwhile, the differences in other key microorganisms between simulative results and actual/field/in situ results are generally less than 5% for both processes. Therefore, the model simulation can accurately predict the amount of methanogens and other microorganisms. Previously, Lee et al. verified methanogen growth in an oxic soil microcosm, and the result could prove that methanogens could grow in an oxic environment [53]. Therefore, methanogens could grow in oxic and anoxic tanks of WWTPs. The model simulative results also show that methanogen WWTPs are mainly from the accumulation of methanogens in the influent, and less methanogens grow in wastewater treatment systems. Therefore, the higher the percentage of methanogens in influent and the longer the sludge retention time (SRT) employed in the wastewater treatment system, the higher the percentage of methanogens in activated sludge when the system is stable. The results explain why there are more methanogens in the Orbal oxidation ditch process without a primary settling tank. In this study, VB6.0 was used to compile simulation software. The initial value of the parameters is the typical parameter values of ASM1, ASM2D, and ADM2. The measured data of the Orbal oxidation ditch process and A/A/O process were used to calibrate the composite model equation that was used to simulate calculation. These results proved that the composite model can simulate methanogen growth in WWTPs well.

Table 6. The percentage (%) of three kinds of bacteria in the sludge from two WWTPs.

	Bacteria	Simulative Result	Actual/Field/In Situ Results	Relative Error
Orbal oxidation ditch	Methanogens	3.45%	3.35%	2.39%
	Ammonia-Oxidizing Bacteria (AOB) and Nitrite-Oxidizing Bacteria (NOB)	3.59%	3.60%	0.28%
	Polyphosphate-Accumulating Organisms (PAOs)	6.48%	6.32%	2.53%
A/A/O	Methanogens	1.92%	1.95%	1.54%
	Ammonia-Oxidizing Bacteria (AOB) and Nitrite-Oxidizing Bacteria (NOB)	4.64%	4.90%	5.31%
	Polyphosphate-Accumulating Organisms (PAOs)	9.29%	9.33%	0.43%

Table 7. The percentage (%) of soluble solids used by methanogen growth.

	Simulative Results	Actual/Field/In Situ Results	Relative Error
Orbal oxidation ditch	2.97%	3.39%	12.39%
A/A/O	0.29%	0.32%	9.38%

3.7. Release Mechanism of Methane Emission from WWTP

How was methane emitted from WWTPs? To determine the underlying mechanism, we construct a physical model to describe methane generation and emission from WWTPs (Figure 8). In the WWTPs, methanogens, which are strictly and obligatory anaerobic organisms, may be located inside sludge flocs. In the anaerobic tank, methanogens convert hydrogen and acetic acid, which were produced by hydrolyzing bacteria and fermenting bacteria, into methane. In anaerobic tanks, all methanogens are in the anaerobic zone. With the increase in dissolved oxygen concentration, the area of the anaerobic zone inside of the sludge flocs decreases. In the anoxic tank and aerobic tank, the methanogens inside the floc remain under anaerobic conditions, which benefits methane generation, because bacteria outside the floc consume dissolved oxygen. Methane is rapidly emitted from wastewater because of the poor solubility of this gas in water. In the aerobic tank, the intensive mechanical aeration strip dissolved methane from water. Therefore, relatively more methane is emitted from the anaerobic tank and aerobic tank.

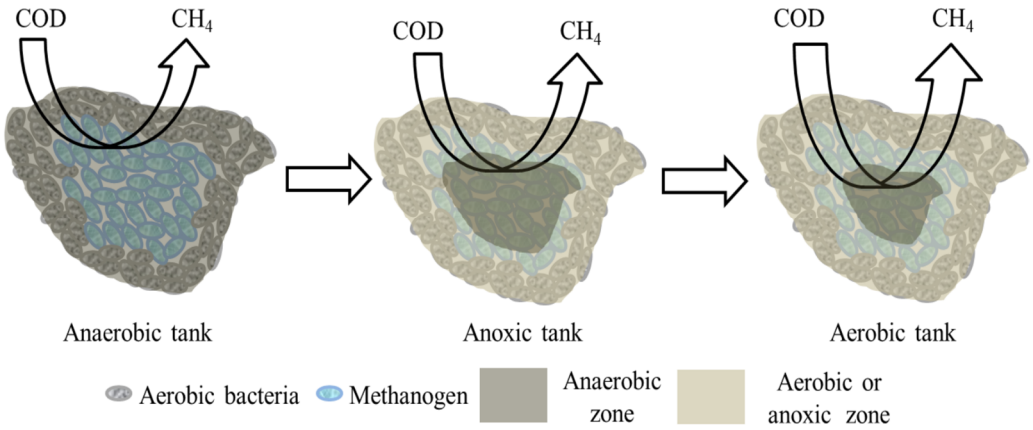

Figure 8. Model for describing methane generation and emission from WWTPs.

4. Conclusions

In conclusion, both BNR processes emitted a larger amount of methane in summer (Jun to Aug, 26.29–30.16 g CH_4 /(m^2 · d)) for the Orbal oxidation ditch and 11.02–14.30 g CH_4 /(m^2 · d) for A/A/O) than in winter (Dec to Feb, 13.65–16.37 g CH_4 /(m^2 · d)) for the Orbal oxidation ditch and 7.78–8.28 g CH_4 /(m^2 · d) for A/A/O). The amount of CH_4 emitted from the Orbal oxidation ditch process was higher than that from the A/A/O process. In the Orbal oxidation ditch, the CH_4 emission flux was 22.74 g CH_4 /(m^2 · d), and emission factors were 1.18 g CH_4 /(m^3 INF) and 64.67 g CH_4 /(person · year), which were 2.4 and 5.6 times higher than those in the A/A/O process (flux: 9.57 g CH_4 /(m^2 · d), factors: 0.21 g CH_4 /(m^3 INF) and 11.44 g CH_4/(person · year). Based on the results of SMA, F_{420} concentration, and the FISH test, the higher methanogenic potential activity of methanogens in the Orbal oxidation ditch led to higher CH_4 emissions. This is supported by the simulative results of methanogens in the model, which can also accurately predict the amount of other key microorganisms in the WWTPs' sludge. Overall, this study provides a basis for establishing a database of CH_4 emissions from WWTPs in China and prove that a primary settling tank could reduce CH_4 emission.

Author Contributions: Conceptualization, H.L.; methodology, H.L. and D.A.; formal analysis, H.L.; investigation, H.L. and X.L.; resources, N.W.; data curation, D.Z. and X.L.; writing—original draft, D.Z.; writing—review and editing, H.L.; visualization, D.Z.; supervision, H.L.; project administration, H.L. All authors have read and agreed to the published version of the manuscript.

Funding: This research was supported by the Scientific Research Program Funded by Shaanxi Provincial Education Department (Program No. 21JK0663); Development Program of Shaanxi, China (Program No. 2019ZDLSF06-05); National Natural Science Foundation of China (Program No. 52100198); Doctoral Research Project fund of Xi'an Polytechnic University.

Data Availability Statement: Data are contained within the article.

Acknowledgments: The authors also appreciated the technical assistance of the staff of the two wastewater treatment plants. We would like to thank Wenbo Liu, Liming Wang, and Min Gao for their assistance in reviewing the first draft and selecting the proper journal.

Conflicts of Interest: Author Na Wang was employed by the company Xi'an Capital Water Co., Ltd. The remaining authors declare that the research was conducted in the absence of any commercial or financial relationships that could be construed as a potential conflict of interest.

References

1. Li, X.J.; Li, J.; Ni, P.J. The Impact of the Digital Economy on CO_2 Emissions: A Theoretical and Empirical Analysis. *Sustainability* **2021**, *13*, 7267–7281. [CrossRef]
2. Hao, C.H.; Fu, X.; Jiang, X.Y.; Li, Y.T.; Sun, J.Y.; Wu, H.T.; Zhu, H.; Li, Q.; Li, Y.H.; Huang, Z.C.; et al. Greenhouse Gas Detection Based on Infrared Nanophotonic Devices. *IEEE Open J. Nanotechn.* **2023**, *4*, 10–22. [CrossRef]
3. Mohanakrishnan, J.; Gutierrez, O.; Meyer, R.L.; Yuan, Z. Nitrite effectively inhibits sulfide and methane production in a laboratory scale sewer reactor. *Water Res.* **2008**, *42*, 3961–3971. [CrossRef]
4. Goliopoulos, N.; Mamais, D.; Noutsopoulos, C.; Dimopoulou, A.; Kounadis, C. Energy Consumption and Carbon Footprint of Greek Wastewater Treatment Plants. *Water* **2022**, *14*, 320–331. [CrossRef]
5. Aghabalaei, V.; Nayeb, H.; Mardani, S.; Tabeshnia, M.; Baghdad, M. Minimizing greenhouse gases emissions and energy consumption from wastewater treatment plants via rational design and engineering strategies: A case study in Mashhad, Iran. *Energy Rep.* **2023**, *9*, 2310–2320. [CrossRef]
6. Gülşen, H.; Yapıcıoğlu, P. Greenhouse gas emission estimation for a UASB reactor in a dairy wastewater treatment plant. *Int. J. Global. Warm.* **2019**, *17*, 373–388. [CrossRef]
7. Du, W.J.; Lu, J.Y.; Hu, Y.R.; Xiao, J.X.; Yang, C.; Wu, J.; Huang, B.C.; Cui, S.; Wang, Y.; Li, W.W. Spatiotemporal pattern of greenhouse gas emissions in China's wastewater sector and pathways towards carbon neutrality. *Nat. Water* **2023**, *1*, 166–175. [CrossRef]
8. Rashid, S.S.; Liu, Y.Q. Assessing environmental impacts of large centralized wastewater treatment plants with combined or separate sewer systems in dry/wet seasons by using LCA. *Environ. Sci. Pollut. Res.* **2020**, *27*, 15674–15690. [CrossRef]
9. Qmbar, A.S.; Khalidy, M.M. Optimizing dissolved oxygen requirement and energy consumption in wastewater treatment plant aeration tanks using machine learning. *J. Water Process Eng.* **2022**, *50*, 103237. [CrossRef]
10. Wang, J.Q.; Hua, M.; Cai, C.Y.; Hu, J.J.; Wang, J.R.; Yang, H.R.; Ma, F.; Qian, H.F.; Zheng, P.; Hu, B.L. Spatial-Temporal Pattern of Sulfate-Dependent Anaerobic Methane Oxidation in an Intertidal Zone of the East China Sea. *Appl. Environ. Microb.* **2019**, *85*, e02638-18. [CrossRef]
11. Hilts, A.S.; Hunjan, M.S.; Hug, L.A. Adapting Macroecology to Microbiology: Using Occupancy Modeling to Assess Functional Profiles across Metagenomes. *Msystems* **2021**, *6*, e00790-21. [CrossRef]
12. Su, G.Y.; Zopfi, J.; Niemann, H.; Lehmann, M.F. Multiple Groups of Methanotrophic Bacteria Mediate Methane Oxidation in Anoxic Lake Sediments. *Front. Microbiol.* **2022**, *13*, 864630. [CrossRef]
13. Arthur, P.M.A.; Konaté, Y.; Sawadogo, B.; Sagoe, G.; Dwumfour-Asare, B.; Ahmed, I.; Williams, M.N.V. Performance evaluation of a full-scale upflow anaerobic sludge blanket reactor coupled with trickling filters for municipal wastewater treatment in a developing country. *Heliyon* **2022**, *8*, e10129. [CrossRef]
14. Wang, J.H.; Zhang, J.; Xie, H.J.; Qi, P.Y.; Ren, Y.G.; Hu, Z. Methane emissions from a full-scale A/A/O wastewater treatment plant. *Bioresour. Technol.* **2011**, *102*, 5479–5485. [CrossRef]
15. Song, C.H.; Zhu, J.J.; Willis, J.L.; Moore, D.P.; Zondlo, M.A.; Ren, Z.Y.J. Methane Emissions from Municipal Wastewater Collection and Treatment Systems. *Environ. Sci. Technol.* **2023**, *57*, 2248–2261. [CrossRef]
16. Aboobakar, A.; Jones, M.; Vale, P.; Carmell, E.; Dotro, G. Methane Emissions from Aerated Zones in a Full-Scale Nitrifying Activated Sludge Treatment Plant. *Water Air Soil Pollut.* **2013**, *225*, 1814. [CrossRef]
17. Xu, Y.; Geng, H.; Chen, R.J.; Liu, R.; Dai, X.H. Enhancing methanogenic fermentation of waste activated sludge via isoelectric-point pretreatment: Insights from interfacial thermodynamics, electron transfer and microbial community. *Water Res.* **2021**, *197*, 117072. [CrossRef]
18. Guisasola, A.; de Haas, D.; Keller, J.; Yuan, Z. Methane formation in sewer systems. *Water Res.* **2008**, *42*, 1421–1430. [CrossRef]

19. Ni, B.J.; Ruscalleda, M.; Pellicer-Nàcher, C.; Smets, B.F. Modeling nitrous oxide production during biological nitrogen removal via nitrification and denitrification: Extensions to the General ASM Models. *Environ. Sci. Technol.* **2011**, *45*, 7768–7776. [CrossRef]
20. Ni, B.J.; Peng, L.; Law, Y.; Guo, J.; Yuan, Z. Modeling of nitrous oxide production by autotrophic ammonia-oxidizing bacteria with multiple production pathways. *Environ. Sci. Technol.* **2014**, *48*, 3916–3924. [CrossRef]
21. Gulhan, H.; Cosenza, A.; Mannina, G. Modelling greenhouse gas emissions from biological wastewater treatment by GPS-X: The full-scale case study of Corleone (Italy). *Sci. Total Environ.* **2023**, *905*, 167327. [CrossRef] [PubMed]
22. Shahabadi, M.B.; Yerushalmi, L.; Haghighat, F. Estimation of greenhouse gas generation in wastewater treatment plants—Model development and application. *Chemosphere* **2010**, *78*, 1085–1092. [CrossRef] [PubMed]
23. *GB 18918-2002*; Discharge Standard of Pollutants for Municipal Waste-Water Treatment Plant. Ministry of Ecological Environment of the People's Republic of China: Beijing, China, 2002.
24. Chandran, K. *Characterization of Nitrogen Greenhouse Gas Emissions from Wastewater Treatment BNR Operations: Field Protocol with Quality Assurance Plan*; Water Environment Research Foundation: Alexandria, VA, USA, 2009.
25. APHA. *Standard Methods for the Examination of Water and Wastewater*, 21st ed.; Eaton, A.D., Clesceri, L.S., Rice, E.W., Greenberg, A.E., Eds.; American Public Health Association: Washington, DC, USA, 2005.
26. Dong, F.; Zhao, Q.B.; Zhao, J.B.; Sheng, G.P.; Tang, Y.; Tong, Z.H.; Yu, H.Q.; Li, Y.Y.; Harada, H. Monitoring the restart-up of an upflow anaerobic sludge blanket (UASB) reactor for the treatment of a soybean processing wastewater. *Bioresour. Technol.* **2010**, *101*, 1722–1726. [CrossRef] [PubMed]
27. Wu, W.M.; Hu, J.C.; Gu, X.S. Coenzyme F420 in anaerobic sludge and its measurement with spectrophotometry. *China Environ. Sci.* **1986**, *6*, 65–68. (In Chinese)
28. Amann, R.I.; Ludwig, W.; Schleifer, K.H. Phylogenetic identification and in situ detection of individual microbial cell swith out cultivation. *Microbiol. Rev.* **1995**, *59*, 143–169. [CrossRef] [PubMed]
29. Daims, H.; Brühl, A.; Amann, R.; Schleifer, K.H.; Wagner, M. The domainspecific probe EUB 338 is insufficient for the detection of all bacteria: Development and evaluation of a more comprehensive probe set. *Syst. Appl. Microbiol.* **1999**, *22*, 434–444. [CrossRef] [PubMed]
30. Raskin, L.; Stromley, J.M.; Rittmann, B.E.; Stahl, D.A. Group specific 16S rRNA hybridation probes to describe natural communities of methanogens. *App. Environ. Microbiol.* **1994**, *60*, 1232–1240. [CrossRef] [PubMed]
31. Mobarry, B.K.; Wagner, M.; Urbain, V.; Rittmann, B.E.; Stahl, D.A. Phylogenetic probes for analyzing abundance and spatial organization of nitrifying bacteria. *Appl. Environ. Microbiol.* **1996**, *62*, 2156–2162. [CrossRef] [PubMed]
32. Wagner, M.; Rath, G.; Amann, R.I.; Koops, H.P.; Schleifer, K.H. In situ identification of ammonia-oxidizing bacteria. *Syst. Appl. Microbiol.* **1995**, *18*, 251–264. [CrossRef]
33. Pommerening, R.A.; Rath, G.; Koops, H.P. Phylogenetic diversity within the genus nitrosomonas. *Syst. Appl. Microbiol.* **1996**, *19*, 344–351. [CrossRef]
34. Adamczyk, J.; Hesselsoe, M.; Iversen, N.; Horn, M.; Lehner, A.; Nielsen, P.H.; Schloter, M.; Roslev, P.; Wagner, M. The isotope array, a new tool that employs substrate-mediated labeling of rRNA for determination of microbial community structure and function. *Appl. Environ. Microbiol.* **2003**, *69*, 6875–6887. [CrossRef] [PubMed]
35. Wagner, M.; Rath, G.; Koops, H.P.; Flood, J.; Amann, R.I. In situ analysis of nitrifying bacteria in sewage treatment plants. *Water Sci. Technol.* **1996**, *34*, 237–244. [CrossRef]
36. Crocetti, G.R.; Hugenholtz, P.; Bond, P.L.; Schuler, A.; Keller, J.; Jenkins, D.; Blackall, L.L. Identification of poly-phosphate-accumulating organisms and design of 16s rRNA-directed probes for their detection and quantitation. *Appl. Environ. Microbiol.* **2000**, *66*, 1175–1182. [CrossRef] [PubMed]
37. Jadeja, N.B.; Ganorkar, R. Mathematical Modelling for Understanding and Improving the Anaerobic Digestion Process Efficiency. In *Anaerobic Biodigesters for Human Waste Treatment*; Environmental and Microbial Biotechnology; Meghvansi, M.K., Goel, A.K., Eds.; Springer: Singapore, 2022; pp. 39–56.
38. Henze, M.; Gujer, W.; Mino, T.; van Loosedrecht, M. *Activated Sludge Models ASM1, ASM2, ASM2d and ASM3*; IWA Publishing: London, UK, 2006.
39. Zaghloul, M.S.; Achari, G. A review of mechanistic and data-driven models of aerobic granular sludge. *J. Environ. Chem. Eng.* **2022**, *10*, 107500. [CrossRef]
40. Zhang, X.H.; Nan, J.; Liu, T.; Xiao, Q.L.; Liu, B.H.; He, X.; Ngo, H.H. Modeling and simulation of an extended ASM2d model for the treatment of wastewater under different COD: N ratio. *J. Water Process Eng.* **2021**, *40*, 101831. [CrossRef]
41. Daelman, M.R.J.; van Voorthuizen, E.M.; van Dongen, U.G.J.M.; Volcke, E.I.P.; van Loosdrecht, M.C.M. Methane emission during municipal wastewater treatment. *Water Res.* **2012**, *46*, 3657–3670. [CrossRef] [PubMed]
42. Speight, J.G. *Lange's Handbook of Chemistry*, 16th ed.; McGraw-Hill, Inc.: New York, NY, USA, 2004.
43. Bitton, G. *Wastewater Microbiology*, 3rd ed.; Wiley-Liss: New York, NY, USA, 2005.
44. Yan, X.; Li, L.; Liu, J.X. Characteristics of greenhouse gas emission in three full-scale wastewater treatment processes. *J. Environ. Sci.* **2014**, *26*, 256–263. [CrossRef] [PubMed]
45. Yan, X.; Cheng, X.; Lun, X.X.; Sun, D.Z. CH_4 emission and conversion from A^2O and SBR processes in full-scale wastewater treatment plants. *J. Environ. Sci.* **2014**, *26*, 224–230. [CrossRef] [PubMed]
46. Sarada, R.; Joseph, R. Studies on factors influencing methane production from tomato-processing waste. *Bioresour. Technol.* **1994**, *47*, 55–57. [CrossRef]

47. Hanson, R.S.; Hanson, T.E. Methanotrophic bacteria. *Microbiol. Rev.* **1996**, *60*, 439–471. [CrossRef]
48. Maya-Altamira, L.; Baun, A.; Angelidaki, I.; Schmidt, J.E. Influence of wastewater characteristics on methane potential in food-processing industry wastewaters. *Water Res.* **2008**, *42*, 2195–2203. [CrossRef] [PubMed]
49. Chen, T.H.; Hashimoto, A.G. Effects of pH and substrate: Inoculum ratio on batch methane fermentation. *Bioresour. Technol.* **1996**, *56*, 179–186. [CrossRef]
50. Liu, Y.W.; Ni, B.J.; Sharma, K.R.; Yuan, Z.G. Methane emission from sewers. *Sci. Total Environ.* **2015**, *524–525*, 40–51. [CrossRef] [PubMed]
51. Banihani, Q.; Sierra-Alvarez, R.; Field, J.A. Nitrate and nitrite inhibition of methanogenesis during denitrification in granular biofilms and digested dometic sludges. *Biodegradation* **2009**, *20*, 801–812. [CrossRef] [PubMed]
52. Jiang, G.M.; Gutierrez, O.; Sharma, K.R.; Yuan, Z. Effects of nitrite concentration and exposure time on sulfide and methane production in sewer system. *Water Res.* **2010**, *44*, 4241–4251. [CrossRef] [PubMed]
53. Lee, C.G.; Watanabe, T.; Murase, J.; Asakawa, S.; Kimura, M. Growth of methanogens in an oxic soil microcosm: Elucidation by a DNA-SIP experiment using 13C-labeled dried rice callus. *Appl. Soil Ecol.* **2012**, *58*, 37–44. [CrossRef]

Disclaimer/Publisher's Note: The statements, opinions and data contained in all publications are solely those of the individual author(s) and contributor(s) and not of MDPI and/or the editor(s). MDPI and/or the editor(s) disclaim responsibility for any injury to people or property resulting from any ideas, methods, instructions or products referred to in the content.